Electronic Supplementary Material (ESI) for Chemical Communications
This journal is © The Royal Society of Chemistry 2013

Electronic Supplementary Information

Synthesis of heterogeneous enzyme/metal nanoparticles biohybrids in aqueous media and their applications in C-C bond formation and tandem catalysis†

Marco Filice*, Marzia Marciello, Maria P. Morales and Jose M. Palomo*

Table of contents

This journal is © The Royal Society of Chemistry 2013

This journal is © The Royal Society of Chemistry 2013

Experimental Section

Materials

Reagents and solvents were obtained from Panreac Quimica, Sigma-Aldrich, Novozymes, Alfa Aesar Gmbh, Thermo Scientific and Toronto Research Chemicals and used without further purification. Inductively coupled plasma atomic emission spectrometry (ICP-AES) was performed on a Perkin Elmer OPTIMA 2100 DV equipment. X-ray photoelectron analysis (XPS) was carried out on SPECS GmbH spectrometer equipped with Phoibos 150 9MCD energy analyzer. A nonmonochromatic magnesium X-ray source with a power of 200 W and voltage of 12 kV was used. The X-Ray diffraction (XRD) pattern was obtained using a Texture Analysis Diffractometer D8 Advance (Bruker) with Cu Kα radiation. The transmission electron microscopy (TEM), high resolution TEM microscopy (HRTEM) and energy dispersive X-ray analysis (EDX) analysis were performed on a JEOL 2100F microscope equipped with an EDX detector INCA x-sight (Oxford Instruments). The scanning electron microscopy (SEM) imaging was performed on a TM-1000 (Hitachi) microscope. The TGA was performed with EXSTAR 6300 (Seiko) equipment in a range of temperature: R. T. / 1000 º C. FTIR spectra were recorded on FT-IR 20SXC (Nicolet) spectrophotometer. The isoelectric point was measured with a Zetasizer Nano S (Malvern Instruments). To recover the biohybrids, a Biocen 22 R (Orto-Alresa, Spain) refrigerated centrifuge was used. The spectrophotometric analyses were run on a V-630 spectrophotometer (JASCO, Japan). HPLC spectrum P100 (Thermo Separation products) was used. Analyses were run at 25°C using an L-7300 column oven and a UV6000LP detector. Column chromatography was carried out on silica gel (Silica gel 60, from Merck, Germany). TLC analysis was performed on Merck silica gel 60 F_{254}. The CALB structure analysis was performed using the PyMOL (DeLano Scientific) software.

This journal is © The Royal Society of Chemistry 2013

General synthesis of CALB/Noble metals nanobiohybrids.

When fully aqueous soluble metal salts were tested (Na_2PdCl_4, $HAuCl_4$ or $AgNO_3$), a solution of the salt in different concentrations (mg/mL) was directly prepared in distilled water (generally 5 mL). When the synthesis of the biohybrids was tested in presence of different organic co-solvents (DMSO, DMF, ACN, MeOH, THF or *i*-PrOH), in the case of $Pd(OAc)_2$, a solution of the salt was firstly prepared in 1 mL of each co-solvent and subsequently was quickly added to 4 mL of distilled water, under vigorous magnetic stirring at 25 °C. The presence of 20% (v/v) of organic co-solvent was necessary to ensure the full dissolution in aqueous medium of 1 mg/mL of $Pd(OAc)_2$. No aggregation was observed in the enzyme solution without Pd salt (>99% of protein amount by Bradford method). NPs formation was not detected using the $Pd(OAc)_2$ solution in the absence of the enzyme, even after centrifugation. For $HAuCl_4$ or $AgNO_3$, the metal salt amount (mg/mL) was directly added to an aqueous solution containing 20% (v/v) of the desired co-solvent. Subsequently, in all the cases, to the newly formed solution, 0.5 mL (2.7 mg of lipase) of *Candida antarctica* fraction B lipase commercial extract (**1**; total lipase concentration: 5.4 mg_{CALB} / mL by Bradford's assay) were added. The final solution was kept on gentle magnetic stirring for 24 h at 25 °C and the formation yields were checked by protein titration of the supernatants (by Bradford's assay in the case of Pd and Ag salts and by the BCA (Bicinchoninic acid) assay when $HAuCl_4$ was used (due to the interference of Au^{3+} with the Coomassie reactant)). The resulting final suspension was separated by centrifugation (10,000 rpm; 4 °C; 20 min) and the recovered pellet was washed two times with the respective synthetic solution (5 mL of distilled water or 5 mL of an aqueous solution containing 20% (v/v) of each organic cosolvent used) and finally two times with distilled water (5 mL for all the preparations). After the last addition of distilled water the suspension was directly lyophilized to obtain the different solid biohybrids

This journal is © The Royal Society of Chemistry 2013

for the further physical characterization (XRD, SEM, TGA, FTIR and XPS). To perform EDX, ζ–potential measures, TEM microscopy and the catalytic reactions, the nanocatalyst suspension in distilled water was directly used.

This general method was totally reproducible obtaining similar amounts by triplicate for each hybrid nanocatalyst prepared.

Discussion on nanobiohybrid formation mechanism.

The two steps mechanism (Scheme S1, initial fast precipitation of cross-linked metal ions-protein complexes followed by spontaneous reduction of metals to their atomic state) involved during the nanobiohybird formation can be explained considering some properties of amino acids or small peptides as it has been described in literature.[1] In fact, the metal binding and reducing ability of free amino acids and tailor-made synthetic small peptides has been deeply investigated.[1] Many parameters have been analyzed finally getting to some general rules that mainly indicate the precise amino acid sequence composition as key-element to obtain the formation of nanomaterials. More in detail, an ideal peptide sequence must present amino acids with moderate binding affinity for both metal ions and formed metal particles (i.e. amino acids presenting hydrophobic or charged side chains (with the charge sign opposite to that showed by the metal ions)) together with neighboring amino acids showing a strong reducing ability (i.e. especially amino acids presenting hydrophobic side chains).[1] Thus, keeping in mind such general rules described for tailor-made peptide synthesis and considering an enzyme as a complex structure of poly-peptide chains, the CALB sequence has been analyzed searching for some naturally present binding/reducing sequences. Effectively, as shown in Figure S10, the enzyme surface contains many peptide sequences possessing the desired binding/reducing activities, especially on its lateral and rear sides (respect to the catalytic site entrance).

This journal is © The Royal Society of Chemistry 2013

Consequently, with all these evidence in our hands, a plausible formation mechanism was postulated (Scheme S1). Adding the metal salt to the enzyme solutions, due to the binding ability of the identified sequences, a rapid adsorption of soluble Me^{n+} ions on the enzyme surface was observed. Furthermore, the adsorbed metal ions act as a cross-linker between the enzyme's molecules, reducing their solubility and finally inducing the initial fast precipitation (Scheme S1, step II). This idea was supported by the evidence that the precipitation phenomenon was also depending on the metal salt concentration in the solution (Table S1 and S2). Once brought closer to the hydrophobic reducing amino acids (for example, Trp (W, 5), Tyr (Y, 9), Phe (F, 10) are present in the CAL-B structure), the metal ions can be therefore reduced to their metallic state (nucleation)(Scheme S1, step III). As demonstrated by the FTIR and ζ-potential analyses of formed nanobiohybrids (Figure S5), this step can be also strengthened by the reductive ability of polyols, as described in literature (due, for example in this case, to the presence of hydroxyl residues of Ser (31) and Thr (37) in the CAL-B structure).[2-3] Finally, deposition of continuously formed metal atoms on the previously generated metal nuclei surface lead to the nanoparticle growth (Scheme S1, step IV).

Enzymatic hydrolysis of 4-nitrophenyl butyrate (1).

In a quartz cuvette containing NaH_2PO_4 pH 7 buffer (0.025 M; 2.5 mL), a solution of **1** in ACN (0.05 M; 0.02 mL) was added under magnetic stirring at 25 °C and let to homogenize for 1 min. To initialize the hydrolysis reaction, in the spectrophotometer, the different CALB/metalNPs biohybrid aqueous suspensions were added. The esterase lipase activity was tested by measuring the increase in absorbance at 348 nm (the isosbestic point of **2**) produced by the release of **2** during the time. The recovered enzymatic activity (%) was obtained comparing the obtained values to the catalytic activity expressed by a 0.054 mg_{CALB}/mL water solution.

This journal is © The Royal Society of Chemistry 2013

Catalytic reduction of 4-nitrophenol (2) to 4-aminophenol (3).

To an aqueous solution of **2** (0.01 M; 2 mL), solid $NaBH_4$ (0.0008 mol; 0.0302 g) was added to reach a final concentration of 0.4 M (The typical catalytic reaction was performed by adding an excess of NaBH4 (0.4 M) to ensure its constant concentration throughout the reaction and, therefore, to apply a pseudo-first-order kinetic with respect to the product **2** to an aqueous solution of the substrate in the presence of catalysts[4]). In these conditions, upon the addiction of $NaBH_4$, the initial absorbance band of the solution of **2** undergoes to an immediate shift from 317 to 400 nm due to the formation of 4-nitrophenolate ions. Immediately after that, the different CALB/metalNPs biohybrid aqueous suspensions were added under gentle mechanical stirring at 25 ºC. The reaction progress was monitored by taking out an aliquot of the solution (0.02 mL) at different times, diluting it with distilled water (2 mL) and measuring the absorption spectrum between 600 and 200nm in a quartz cuvette.

Domino synthesis of 4-aminophenol (3) from 4-nitrophenyl butyrate (1).

To NaH_2PO_4 pH 7 buffer (0.025 M; 2.25 mL), the solution of **1** in ACN (0.1 M; 0.25 mL) was added under magnetic stirring at 25 °C and let to homogenize. After that, the CALB/PdNPs-5 biohybrid aqueous suspension was added. The reaction was kept on gentle stirring until complete conversion of substrate **1** to product **2** (about 1h). Subsequently, to initialize the Pd-catalyzed reduction of **2** to **3**, solid $NaBH_4$ (0.001 mol; 0.0378 g) was directly added to the reaction mixture under gentle magnetic stirring at 25 ºC. The reaction progress was monitored by taking out an aliquot of the solution (0.02 mL), diluting it with water (2 mL) and measuring the absorption spectrum between 600 and 200nm in a quartz cuvette. The complete conversion of **2** to **3** was achieved in about 1 minute.

This journal is © The Royal Society of Chemistry 2013

General procedure for Suzuki-Miyaura reaction

The aryl halide **4** (chlorobenzene: 0.051 mL, 0.5 mmol; bromobenzene: 0.053 mL, 0.5 mmol; iodobenzene: 0.059 mL, 0.5 mmol) was added to a 1.5 mL screw-sealed vessel containing phenylboronic acid **5** (0.067 g, 0.55 mmol), NaOH (0.03 g, 0.75 mmol) and, where indicated, the PTC (TBAF: 0.043 g, 0.165 mmol; TBACl: 0.046 g, 0.165 mmol; TBABr: 0.054 g, 0.165 mmol) in distilled water (0.9 mL). The mixture was kept at 50 °C under vigorous magnetic stirring for 5 min. After that, to initialize the reaction, the aqueous suspension of the CALB/PdNPs-2 biohybrid (0.8 mg / mL; 0.1 mL; about 130 ppb of Pd) was added. The final suspension was left under vigorous magnetic stirring at 50 °C for the indicated times. The reaction outgoing was monitored by HPLC analysis of the reaction's samples withdrawn at different times. The analysis conditions were performed with a Kromasil-C4 (150 × 4.6 mm and 5 μm Ø), at a flow of 1.5 mL / min; λ: 254 nm; and a mobile phase: 50% (v/v) ACN in MilliQ water. In these conditions the biphenyl product **6** gets an R_t of 9 min. The yields were obtained extrapolating the values through a calibration curve of **6** (R^2=0.9973). Representative kinetic curve of the coupling reaction is reported in Figure S11. To confirm the suitability of the HPLC method, the reactions performed with aryl bromide and iodide in absence of PTC, once reached their maximum conversion, were extracted with Et_2O (3 x 2 mL). The combined filtrate was dried over $MgSO_4$ and concentrated under reduced pressure. The residue was chromatographed on silica-gel (hexane). The yields obtained in each case were in agreement with those obtained by HPLC. Furthermore, the homocoupling of aryl halides and phenyl boronic acid was also investigated and no traces of biphenyl product were observed. To perform the purification by silica-gel chromatography as well as to perform the recyclability studies, the reaction amounts were scaled up five times, maintaining the reactants' proportion as described above. After extraction of the organic compounds with

diethyl ether, the aqueous phase was centrifuged to recover the nanocatalyst and the supernatant removed. A new set of reactants was added over the recovered composite biocatalyst and a new reaction cycle was run. Almost quantitative biphenyl yield was obtained in every cycle and the kinetic parameters of each reaction were very similar among them as also demonstrated by the similar TOF values (Table S5). No traces of Pd (checked by ICP-AES analysis) or protein (checked by Bradford and BCA methods) were found in the supernatant of the reaction after total conversion.

General procedure for Heck reaction

In a 1.5 mL screw-sealed vessel, to a solution containing iodobenzene **7** (0.0306 mL, 0.274 mmol) and ethyl acrylate **8** (0.059 mL, 0.55 mmol) in DMF or DMF/distilled water (final volume 1 ml), 1 mg of nanocatalyst (0.25 mg, 2.35 μmol of Pd, 0.0085 mol% of PdNP) was added. The mixture was preheated at 70 °C under vigorous magnetic stirring for 5 min. After that, to initialize the reaction, triethylamine (0.057 mL, 0.412 mmol) was added. The final suspension was left under vigorous magnetic stirring at 70 °C for the indicated times. The reaction outgoing was monitored by HPLC analysis of the reaction's samples withdrawn at different times. The analysis conditions were performed with a Kromasil-C4 (150 × 4.6 mm and 5 μm Ø), at a flow of 1.5 mL / min; λ: 254 nm; and a mobile phase: 50% (v/v) ACN in MilliQ water. In these conditions the ethyl cinnamate product **9** gets an R_t of 6 min. The yields were obtained extrapolating the values through a calibration curve of the product (R^2=0.9964). Representative kinetic curve of the coupling reaction is reported in Figure S11. To confirm the suitability of the HPLC method, the best reaction performed in the presence of 25 % (v/v) of distilled water, once reached its maximum conversion, was extracted with Et_2O. The combined filtrate was dried over $MgSO_4$, concentrated under reduced pressure and finally purified by silica-gel chromatography (hexane). The yields obtained in each case were in

This journal is © The Royal Society of Chemistry 2013

agreement with those obtained by HPLC. To perform the purification by silica-gel chromatography as well as to perform the recyclability studies, the reaction amounts were scaled up five times, maintaining the reactants' proportion as described above. The E configuration was confirmed by HPLC using the (E) and (Z)-**9** standards.

General procedure for the dynamic kinetic resolution (DKR) of (±)-1-phenylethylamine (10)

The acylating agent (ethyl acetate **11** 6 μl, 0.06 mmol or isopropyl acetate **12** 14 μl, 0.06 mmol) was added to a 1.5 mL screw-sealed vessel containing **10** (1.3 μL, 0.01 mmol) in toluene (1 mL). The mixture was kept at 70 °C under vigorous magnetic stirring for 5 min. After that, to initialize the reaction, 5 mg of lyophilized CALB/PdNPs-5 biohybrid (1 mol% of PdNP/3.75 mg CALB) were added. The final suspension was left under vigorous magnetic stirring at 70 °C for the indicated times. The Pd-catalyzed racemization process was studied using S-**10** as substrate and CALB/PdNPs-4 or CALB/PdNPs-5 as catalysts in the conditions described above.

The reactions were monitored by RP-HPLC analysis of the reaction's samples withdrawn at different times. The analysis conditions were column: Kromasil Ultrabase C18, 250x4.6 mm, 5 μmø; f: 1 mL / min; λ: 210 and 254 nm; mobile phase: 30% (v/v) ACN in MilliQ water 0.1% (v/v) trifluoroacetic acid and temperature: 25 °C. R_t of **10** was 3.24 min whereas R_t of **13** was 7.0 min. The standard reference compounds were obtained after converting the commercial aryl amines to the corresponding amide (R-acetamide, S-acetamide and Rac-acetamide) by treatment with few drops of acetic anhydride into the vial. Before their injection, the different samples were diluted with the mobile phase and centrifuged 10 min at 10k rpm. Each sample was injected in triplicate.

This journal is © The Royal Society of Chemistry 2013

The enantiomeric excess (ee) value was determined by chiral HPLC analysis of the reaction's samples withdrawn at final time. The analysis conditions were: Phenomenex Lux Cellulose-1 (250x4.6 mm, 3 μmø) column, flow of 0.5 mL / min; λ: 210 and 254 nm; mobile phase: 10% (v/v) IPA in n-Hexane and temperature: 25 °C. R_t of S-**13** was 24 min whereas R_t of R-**13** was 26.5 min. Before their injection, the different samples were diluted with the mobile phase and centrifuged 10 min at 10k rpm. Each sample was injected in triplicate.

To perform the recycling studies to produced *R*-**13**, the suspension was centrifuged 10 min at 10k rpm. The recovered catalyst was washed and centrifuged 3 times with 1 ml of toluene and finally used with a new set of reagents as previously described.

This journal is © The Royal Society of Chemistry 2013

Supplementary Scheme

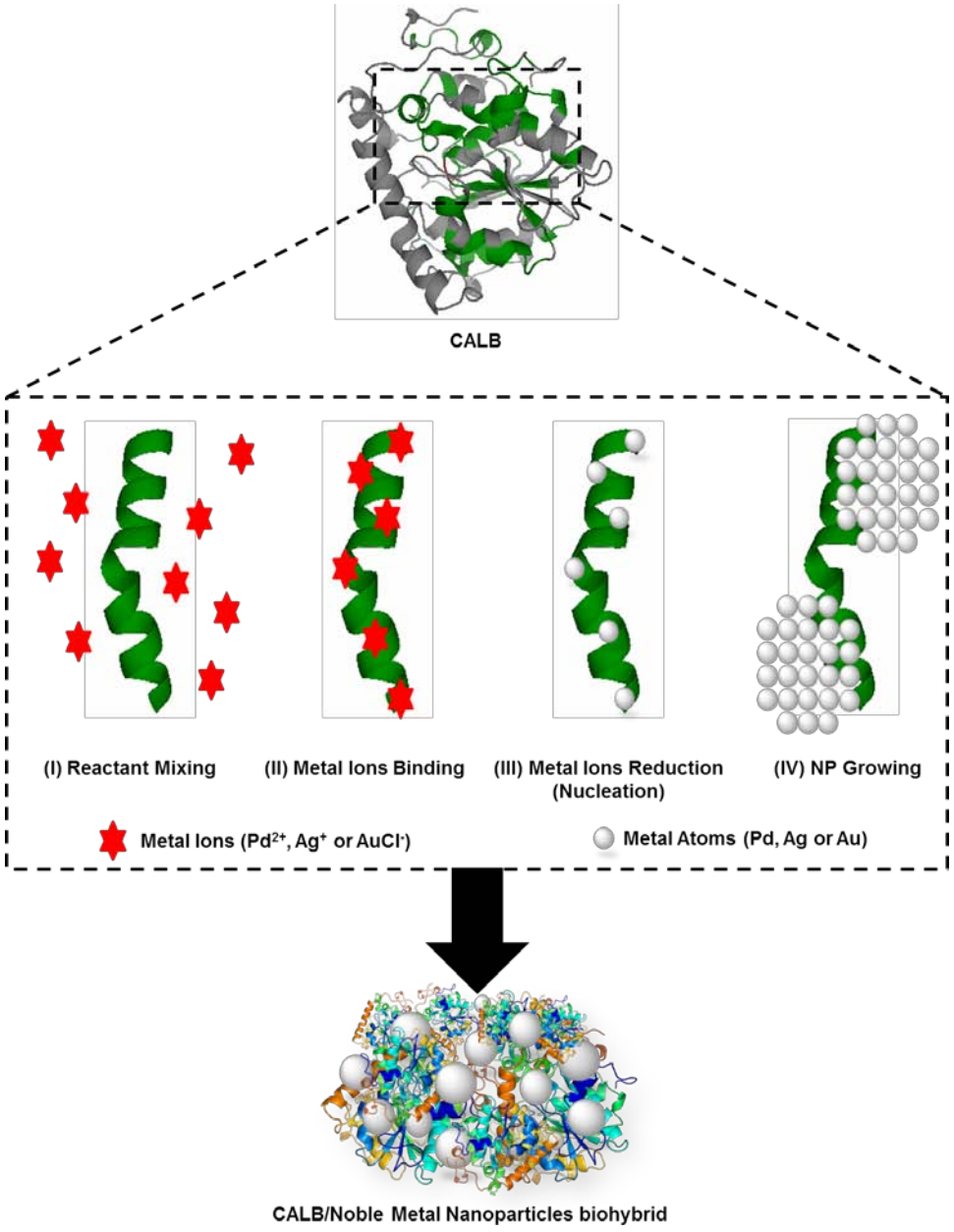

Scheme S1. Proposed model for the nanobiohybrid formation mechanism. (I) The metal salt is added to the enzyme solution; (II) Formation of enzyme-metal ions complexes (cross-linking) thanks to the binding ability of marked peptidic sequences (green); (III) Peptide-mediated reduction of metal ions to metal atoms (nucleation); (IV) Growth of nuclei into crystalline particles.

This journal is © The Royal Society of Chemistry 2013

Supplementary Figures

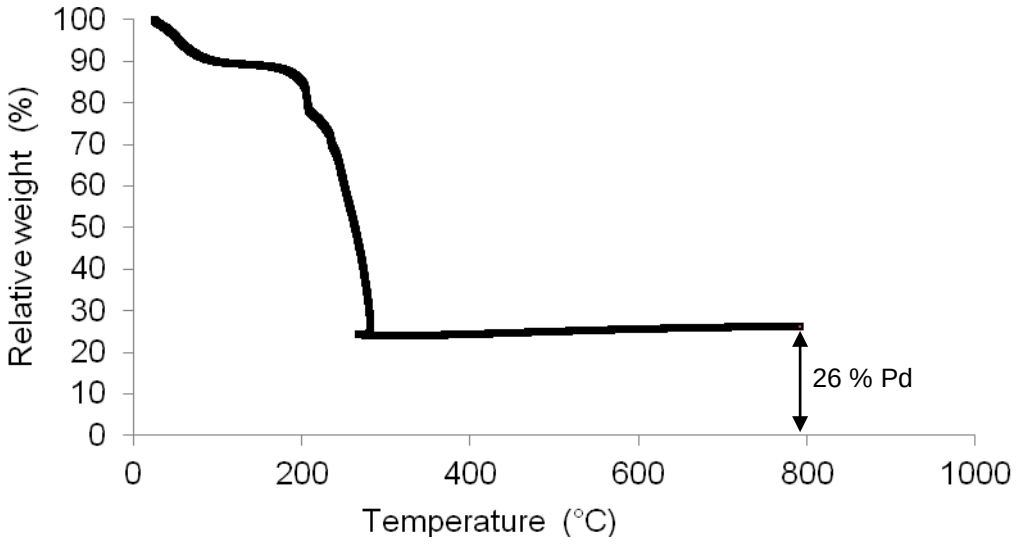

Figure S1. TGA of the CALB/PdNPs-2 biohybrid after 24 h of incubation.

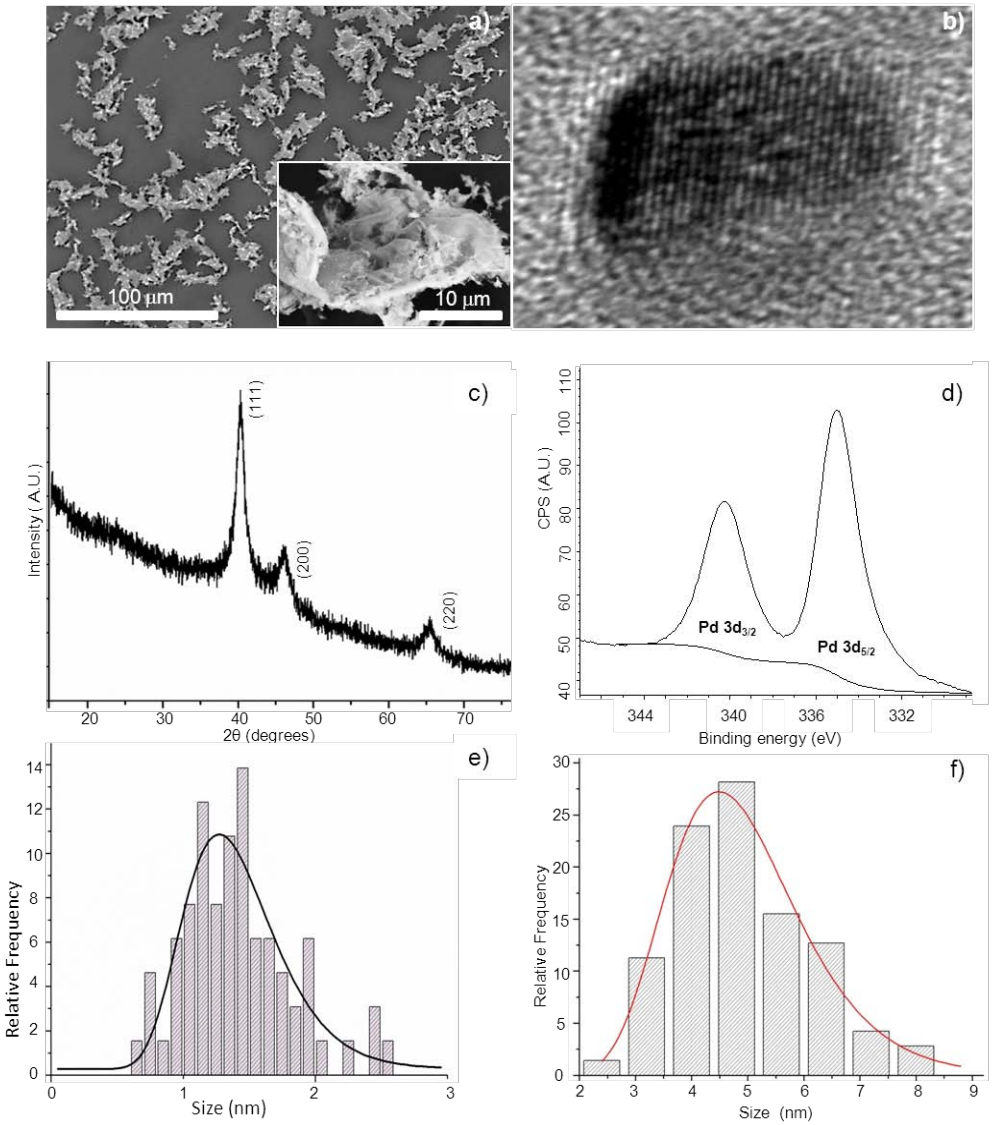

Figure S2. Physicochemical characterization of CALB/PdNPs-2 biohybrid. a) SEM images, b) HRTEM images, c) XRD pattern, d) XPS image, e) smaller PdNPs size distribution, f) larger images PdNPs size distribution. XRD pattern (Figure S2c) showed the presence of a face centered-cubic structure assigned to metal palladium. Mean crystal size calculated from the (111) peak broadening by the Scherrer-Debye formula gives a value of about 5 nm. The broadening of the peaks at the bottom indicates the presence of an important fraction of smaller particles. In XPS (Figure S2d) the presence of a unique $Pd3d_{5/2}$ peak situated at 334 eV undoubtedly confirms the presence of zerovalent Pd specie.

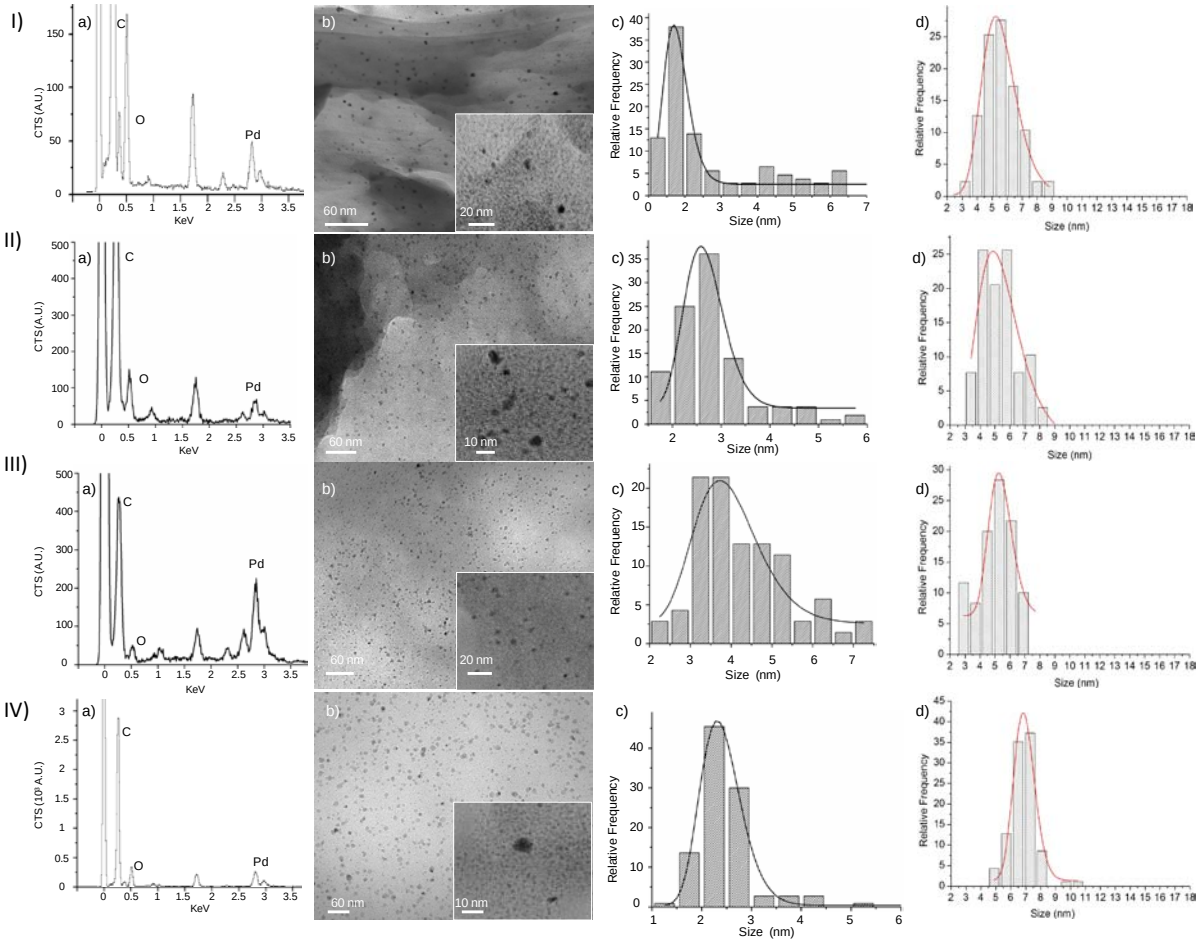

Figure S3. Characterization of CALB/PdNPs (3-6) biohybrids. I) CALB/PdNPs-3, II) CALB/PdNPs-4, III) CALB/PdNPs-5, IV) CALB/PdNPs-6. a) EDX, b) TEM, c) smaller PdNPs size distribution, d) larger images PdNPs size distribution.

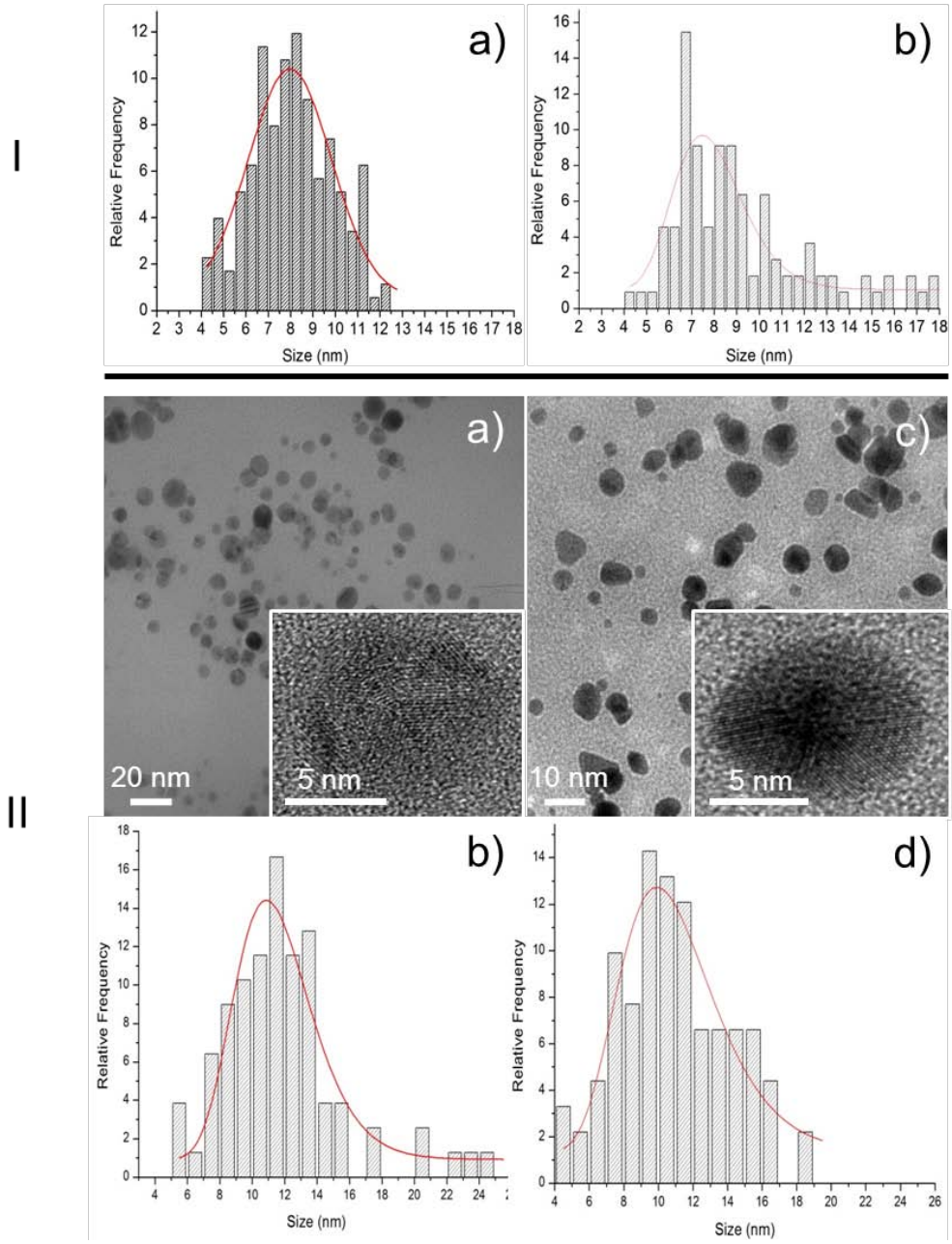

Figure S4. Characterization of CALB/Ag and AuNPs biohybrids. **I:** a) Size distribution of NPs dispersed onto the CALB/AgNPs-1 biohybrid framework; b) Size distribution of NPs dispersed onto the CALB/AuNPs-1 biohybrid framework. **II:** Characterization of CALB/AgNPs-2 biohybrid**:** a) TEM and HRTEM micrographs; b) Size distribution of NPs dispersed onto the CALB/AgNPs framework and CALB/AuNPs-2: c) TEM and HRTEM micrographs; d) Size distribution of NPs dispersed onto the CALB/AuNPs framework.

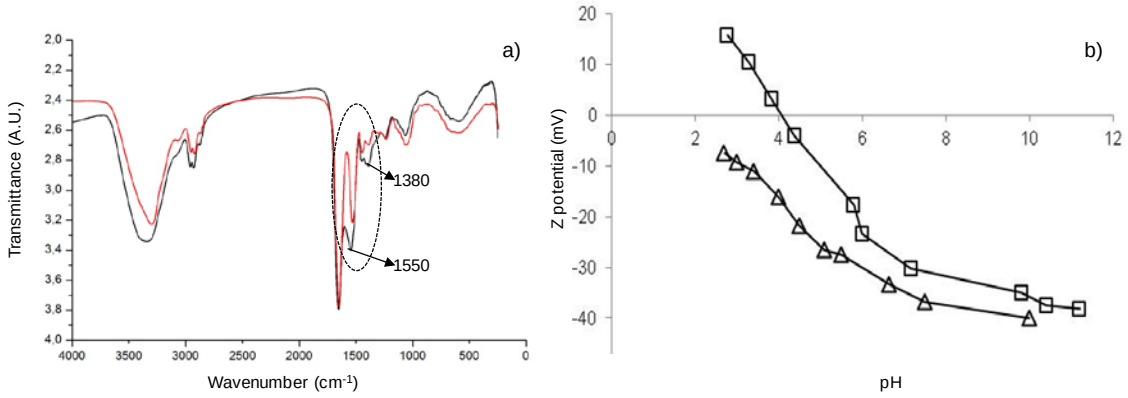

Figure S5. FTIR and ζ-Potential analysis of CALB/PdNPs-2 biohybrid. a) FTIR spectra of CALB before (red) and after (black) the formation of CALB/PdNPs-2 biohybrid. b) Zeta potential of native CALB (squares) and CALB/PdNPs-2 (triangles).

Two signals at ~1550 and 1380 cm-1 in the IR spectrum (1550 cm^{-1}: antisymmetric stretching vibration (ν_{as}) of COO^- of side-chain of Aspartic and Glutamic acid; 1380 cm^{-1}: symmetric stretching vibration (ν_s) of COO^- of side-chain of Aspartic and Glutamic acid)[5] correspond to the presence of higher number of carboxylic groups in the protein (generated by the oxidation of some -OH groups of Ser).[2-3] This result was confirmed by the pH-dependent zeta potential analysis where the isoelectric point (pI) of the biohybrid resulted clearly lower than the pI of native enzyme. Surface charge at pH 7 was around -30 mV which assures long term stability of the colloids.

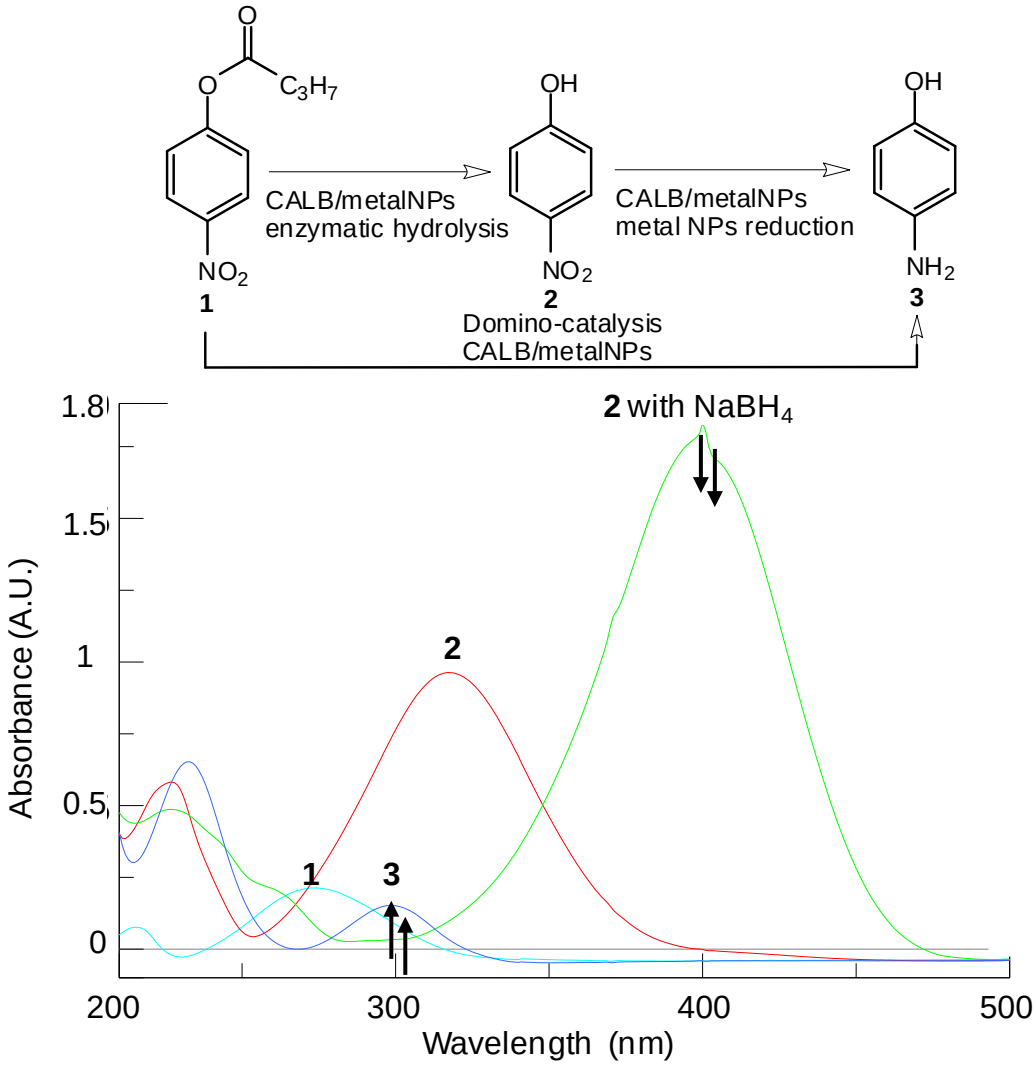

Figure S6. Domino synthesis of **3** from **1**. a) Reaction scheme. b) UV absorption spectra of the reaction. The adsorption peak at 400 nm (corresponding to the concentration of **2**), time-depending quickly decreased in intensity with a contemporary appearance of an increasing shoulder at 300 nm, indicating the reduction of **2** to **3.**

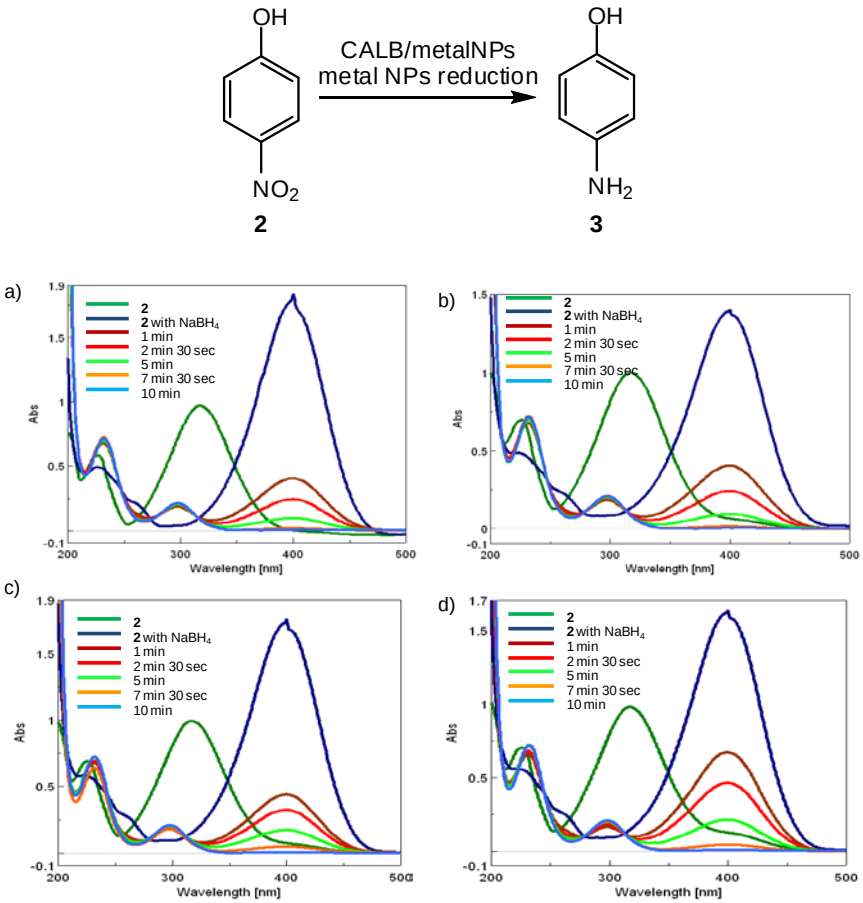

Figure S7. Time-dependent absorption spectra of the metal-catalyzed reduction of **2** in the presence of different nanocatalysts and $NaBH_4$: a) CALB/PdNPs-5; b) CALB/PdNPs-6; c) CALB/AgNPs-1; d) CALB/AuNPs-1.

This journal is © The Royal Society of Chemistry 2013

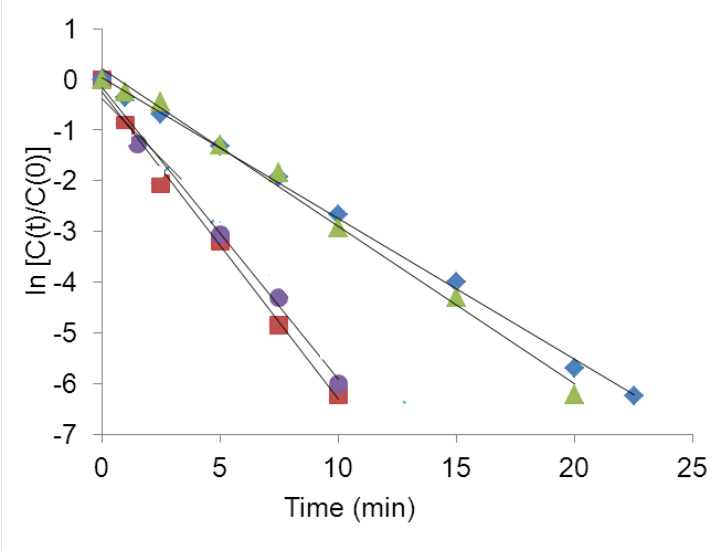

Figure S8. Plot of ln[*C*(*t*)/*C*(0)] against the reaction time. CALB/PdNPs-5 (red square); CALB/PdNPs-6 (purple circle); CALB/AgNPs-1 (blue rhombus), CALB/AuNPs-1(green triangle). The *k* value was calculated performing the linear relationship between ln*C*(*t*)/*C*(0) (with *C*(*t*) and *C*(0) representing the concentration of product **2** at time *t* and 0, respectively) and reaction time.

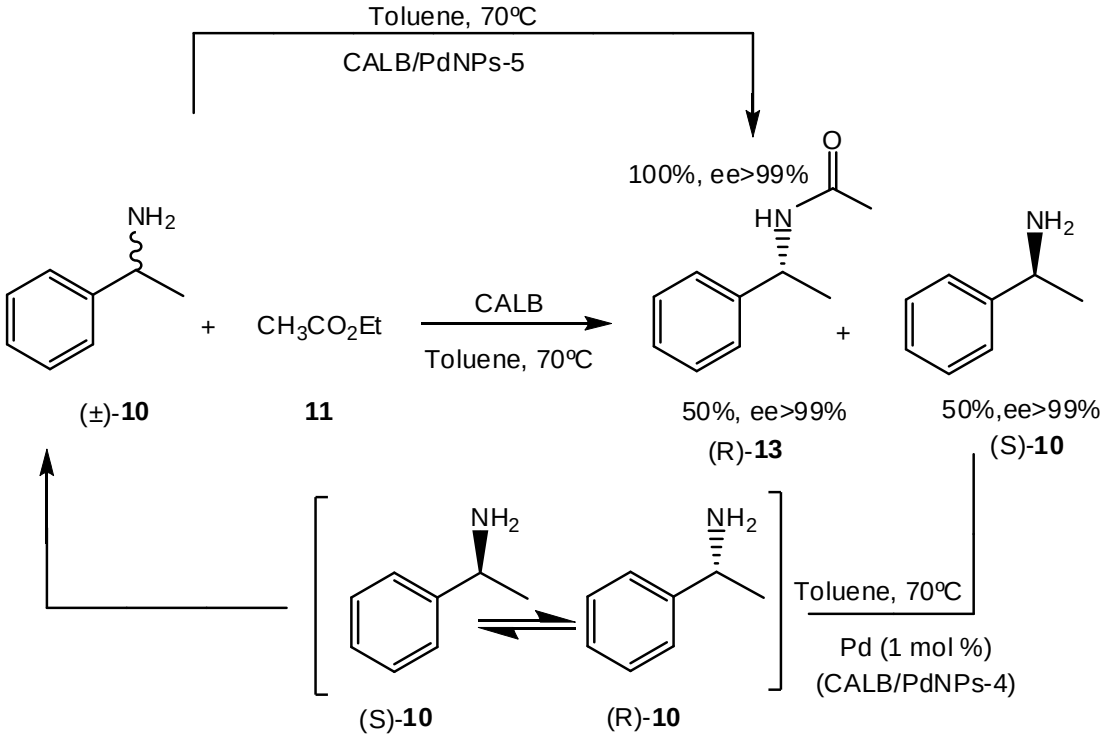

Figure S9. Dynamic kinetic resolution of **10** by enzymatic acetylation, Pd racemization and the overall tandem enzyme-Pd catalysis.

This journal is © The Royal Society of Chemistry 2013

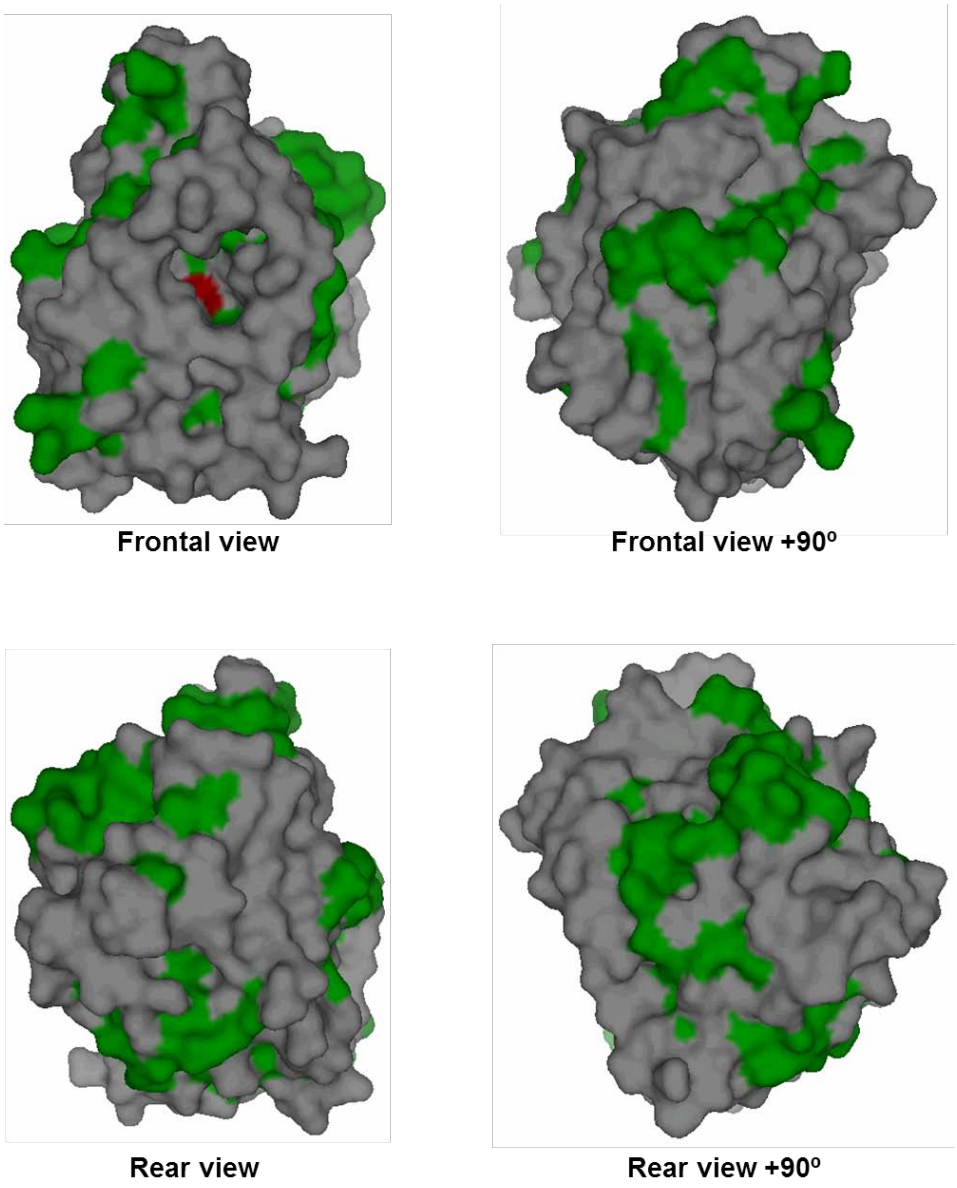

Figure S10. Surface analysis of CALB structure (PDB file: 1TCA). The peptide structures involving amino acid residues possessing binding/reducing ability -useful to form metal nanoparticles- are marked in green (the catalytic Ser105 is marked in red).

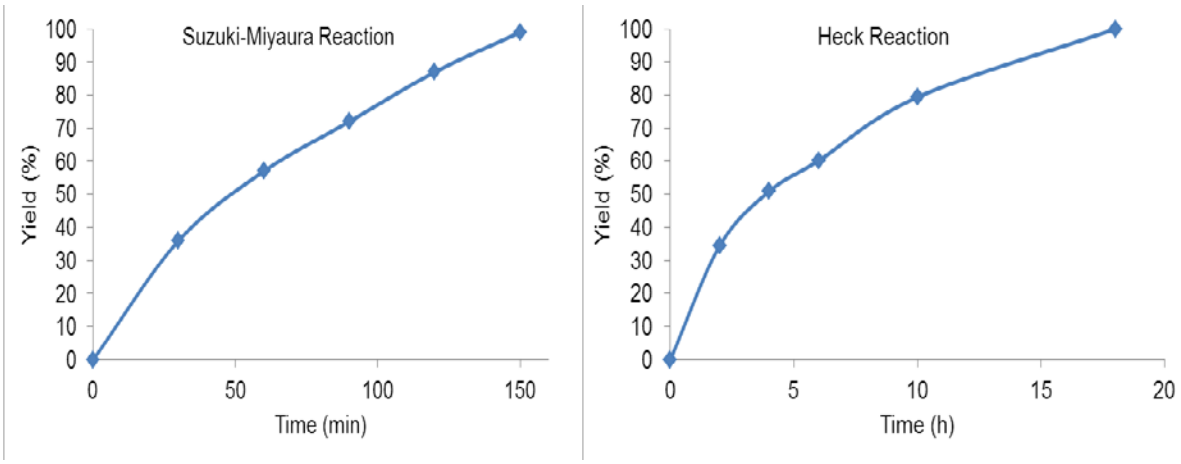

Figure S11. Kinetic curves for Suzuki-Miyaura and Heck coupling reactions.

This journal is © The Royal Society of Chemistry 2013

Supplementary Tables

Table S1: Synthesis of enzyme-Pd nanobiohybrids

Catalyst	Co-Solvent[a]	Metal salt (1 mg/mL)	Protein amount (%)[b]	Metal amount (μmol)[c]
CALB/PdNPs-1	--	Na_2PdCl_4	10	nd
CALB/PdNPs-2	DMF	$Pd(OAc)_2$	99	6.45
CALB/PdNPs-3	DMSO	$Pd(OAc)_2$	99	7.57
CALB/PdNPs-4	ACN	$Pd(OAc)_2$	99	7
CALB/PdNPs-5	MeOH	$Pd(OAc)_2$	99	6.68
CALB/PdNPs-6	THF	$Pd(OAc)_2$	99	7.12
CALB/PdNPs-7	*i*-Propanol	$Pd(OAc)_2$	25	nd

[a] 20% (v/v);[b] The amount of precipitated protein was calculated by Bradford assay of supernatant after 24h. [c] the metal amount disappeared of the solution was calculated by ICP-AES analysis of supernatant after 24h.

This journal is © The Royal Society of Chemistry 2013

Table S2: Synthesis of enzyme-Ag and Au nanobiohybrids

Catalyst	Co-solvent[a]	Metal salt (mg/mL)	Enzyme amount (%)[b]	Metal amount (μmol)[c]
CALB/AgNPs-1	--	$AgNO_3$ (20)	83	41.7
CALB/AgNPs-2	MeOH	$AgNO_3$ (20)	99	37.3
CALB/AgNPs-3	THF	$AgNO_3$ (20)	99	38.5
CALB/AuNPs-1	--	$HAuCl_4$ (10)	93	19.4
CALB/AuNPs-2	MeOH	$HAuCl_4$ (10)	92	18.7
CALB/AuNPs-3	THF	$HAuCl_4$ (10)	93	19.1

[a]20% (v/v);[b] The amount of precipitated protein was calculated by Bradford assay of supernatant after 24h. When $HAuCl_4$ was used, due to the interference with the Coomassie reactant, the BCA (Bicinchoninic acid) protein assay was performed. [c] the metal amount disappeared of the solution was calculated by ICP-AES analysis of supernatant after 24h.

This journal is © The Royal Society of Chemistry 2013

Table S3. Catalytic characterization of enzyme-PdNPs biohybrids

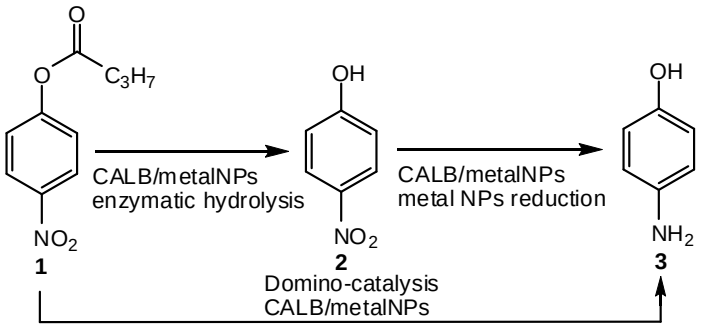

Catalyst	Enzymatic activity (%)[a]	Noble metal-NPs catalytic activity	
		k (min^{-1})[b]	TOF min^{-1}[c]
CALB/PdNPs-2	6.5	nd	nd
CALB/PdNPs-5	47.8	0.6	149.7
CALB/PdNPs-6	45.8	0.58	140.4
CALB/AgNPs-1	<5	0.28	10.6
CALB/AuNPs-1	24.8	0.31	25.7

[a]Compared to the initial activity of CALB solution in absence of metal salts; [b] The k value was calculated performing the linear relationship between $\ln C(t)/C(0)$ (with $C(t)$ and $C(0)$ representing the concentration of product **2** at time t and 0, respectively) and reaction time; [c] The TOF value was defined as the moles of **3** per mole of noble metal atoms in the nanocatalyst per minute.

Table S4: Suzuki-Miyaura coupling of aryl halides with aryl boronic acid catalyzed by CALB/PdNPs-2 biohybrid.[a]

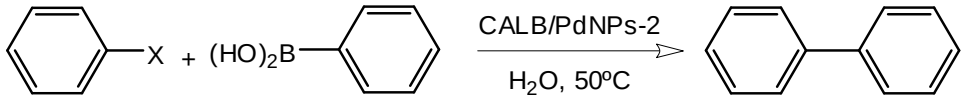

4 **5** **6**

Entry	X	PTC[b]	Base (eq)	Time (h)	Yield (%)[c]
1	Cl	--	NaOH [1.5]	48	2
2	Br	--	NaOH [1.5]	24	50
3	I	--	NaOH [1.5]	24	55
4	Cl	TBAF	NaOH [1.5]	48	1
5	Cl	TBACl	NaOH [1.5]	48	2
6	Cl	TBABr	NaOH [1.5]	48	1
7	Br	TBAF	NaOH [1.5]	10	96
8	Br	TBACl	NaOH [1.5]	2.5	99
9	Br	TBABr	NaOH [1.5]	5	99
10	I	TBAF	NaOH [1.5]	34	51
11	I	TBACl	NaOH [1.5]	38	52
12	I	TBABr	NaOH [1.5]	38	50
13	Cl	TBAF	NaOH [2.0]	48	4
14	Br	TBACl	NaOH [2.0]	48	97
15	I	TBAF	NaOH [2.0]	30	57
16	Cl	TBAF	K_2CO_3 [2.0]	24	20
17	Br	TBACl	K_2CO_3 [2.0]	52	96
18	I	--	K_2CO_3 [2.0]	30	56

[a]Reaction conditions: **4** (0.5 mmol), **5** (0.55 mmol), H_2O (1 mL), 130 ppb of Pd catalyst, 50°C; [b] Phase transfer catalyst; 0.165 mmol; [c] Calculated by HPLC analysis as described in Supporting Information.

This journal is © The Royal Society of Chemistry 2013

Table S5. Recycling ability of the CALB/PdNPs-2 biohybrid in the Suzuki-Miyaura coupling at 50 ºC at maximum conversion.[a]

Cycle	Yield (%)	TOF (h^{-1})[b]
1	99	2137
2	96	2070
3	97	2094
4	93	2007
5	95	2050

[a] Reaction conditions: bromobenzene (2.5 mmol), phenylboronic acid (2.75 mmol), NaOH (1.5 eq.), TBACl (0.33 eq.), H_2O (4.5 mL), 50°C and CALB/PdNPs-2 aqueous suspension (0.37 mg / mL; 0.5 mL). [b] 2.5 h

Table S6: Heck coupling of aryl iodide with ethyl acrylate catalyzed by CALB/PdNPs-4.[a]

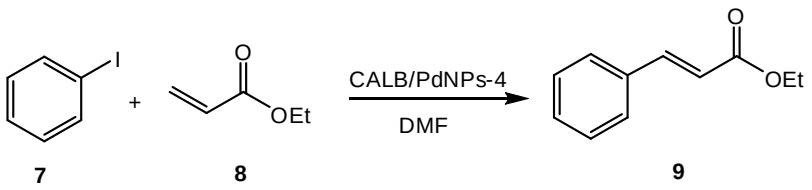

7 **8** **9**

Entry	Co-solvent (%v/v, H_2O)	T (^oC)	Time (h)	Yield (%)[b]
1	--	120	24	99
2	--	60	24	0
3	25	60	24	0
4	50	60	24	0
5	--	70	24	0
6	25	70	18	99
7	50	70	24	20

[a]Reaction conditions: **7** (0.274 mmol), **8** (0.55 mmol), DMF (1 mL), 1 mg of CALB/PdNPs-4 catalyst, 70°C, triethylamine (TEA) (0.412 mmol); [b] Calculated by HPLC analysis as described in Supporting Information

Table S7: Dynamic Kinetic Resolution (DKR) of (±)-1-phenylethylamine (**10**) catalyzed by CALB/PdNPs-5.[a]

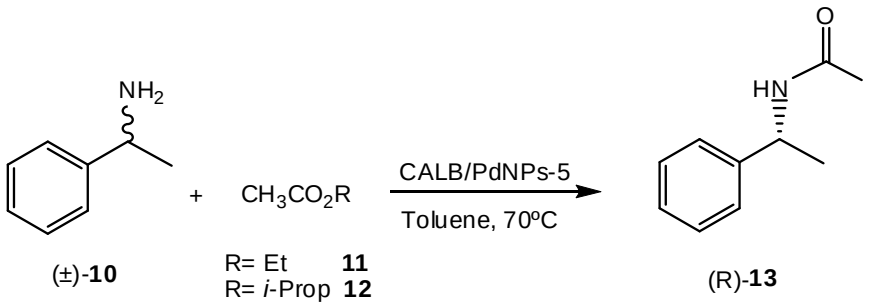

Entry	MS 3Å (w/v)	Base[b]	R	Time (h)	Conversion (%)[c]	ee (%)[d]
CALB/PdNPs-5	-	-	Et	4	98	>99
CALB/PdNPs-5	-	-	$Prop_{iso}$	5	88	90
CALB/PdNPs-5	10	-	Et	4	96	>99
CALB/PdNPs-5	-	TEA	Et	4	91	28
CALB/PdNPs-5	-	DIPEA	Et	5	97	74
CALB/PdNPs-6	-	-	Et	4	98	>99

[a]Reaction conditions: **10**(0.01 mmol), **11** or **12** (0.06 mmol), toluene (1 mL) and 70°C, 5 mg CALB/PdNPs-5. [b] 0.07 mmol. [c] Calculated by RP-HPLC analysis. [d] Determined by chiral HPLC.

Abbreviations: TEA: triethylamine, DIPEA: *N*,*N*-diisopropylethylamine.

This journal is © The Royal Society of Chemistry 2013

Table S8. Racemization process of (S)-**10**.[a]

Entry	Catalyst	Time (h)	ee (%)[b]
1	CALB/PdNPs-4	6	6
2	CALB/PdNPs-4	12	1
3	CALB/PdNPs-5	6	8
4	CALB/PdNPs-5	12	1

[a]Reaction conditions: (S)-**10** (0.01 mmol), Toluene (1 mL), 70°C and 5 mg of nanocatalyst. [b] Determined by chiral HPLC.

This journal is © The Royal Society of Chemistry 2013

Table S9. Recycling ability of the CALB/PdNPs-5 catalyst in the DKR of (±)-1-phenylethylamine **10** at maximum conversion.[a]

Cycle	Yield (%)[b]	ee (%)[c]
1	98	>99
2	96	>99
3	96	>99

[a] Reaction conditions: **10** (0.01 mmol), **11** (0.06 mmol), toluene (1 mL) and 70°C, 5 mg CALB/PdNPs-5. [b] RP-HPLC yields at 4 h. [c] Determined by chiral HPLC.

This journal is © The Royal Society of Chemistry 2013

References

1 Y.T. Tan, J.Y. Lee and D.I.C. Wang, *J. Am. Chem. Soc*. **2010**, 132, 5677 -5686.

2 (a) R.W.J. Scott, O.M. Wilson and R.M. Crooks, *J. Phys. Chem. B* **2005**, 109, 692-704; (b) H. Li, J.K. Jo, L.D. Zhang, C.-S. Ha, H. Suh and I. Kim, *Langmuir* **2010**, 26, 18442-18453

3 P. de la Presa, T. Rueda, M. del Puerto Morales, F. J. Chichon, R. Arranz, J. M. Valpuesta and A. Hernando, *J. Phys. Chem. B* **2009**, 113, 3051-3057.

4 K. Hayakawa, T. Yoshimura and K. Esumi, *Langmuir* **2003**, *19*, 5517-5521

5 A. Barth, *Biochim. Biophys. Acta* 2007, **1767**, 1073-1101.